JOURNAL OF MATERIALS SCIENCE **34** (1999) 5273–5280

Lanthanide oxide-doped titanium dioxide: Effective photocatalysts for the degradation of organic pollutants*

K. T. RANJIT
Institute of Chemistry, and Farkas Center for Light-Induced Processes, The Hebrew University of Jerusalem, Jerusalem 91904, Israel

H. COHEN
Chemical Services Unit, Weizmann Institute of Science, Rehovot 76100, Israel

I. WILLNER‡
Institute of Chemistry, and Farkas Center for Light-Induced Processes, The Hebrew University of Jerusalem, Jerusalem 91904, Israel
E-mail: willnea@vms.huji.ac.il

S. BOSSMANN, A. M. BRAUN
Lehrstuhl für Umweltmesstechnik der Universität Karlsruhe (TH), Engler-Bunte-Institut, Richard-Willstätter-Allee 5, 76128 Karlsruhe, Germany

A series of lanthanide oxide-doped titanium dioxide photocatalysts Ln_2O_3/TiO_2 (Ln^{3+} = Eu^{3+}, Pr^{3+}, Yb^{3+}) were prepared. The photocatalysts reveal a substantially enhanced activity for the degradation of organic pollutants, as compared to undoped TiO_2. The photodegradation processes of *p*-nitrobenzoic acid, (**1**), *p*-chlorophenoxyacetic acid, (**2**), aniline, (**3**), salicylic acid, (**4**), and *trans*-cinnamic acid, (**5**), with the different photocatalysts was examined. The photodegradation of (**1**)–(**5**) is significantly faster with Ln_2O_3/TiO_2 photocatalysts and leads to complete mineralization of the organic compounds. The high activity of the Ln_2O_3/TiO_2 photocatalysts is attributed to the enhanced association of the functionalized organic pollutants to lanthanide-ion surface sites.

1. Introduction

Semiconductor photocatalysts have evoked tremendous interest over the last decade for the light-stimulated degradation of aqueous pollutants [1, 2] and atmospheric pollutants [3, 4]. Photocatalytic remediation of organic pollutants, such as alkanes, alkenes, phenols, carboxylic acids, surfactants and pesticides, was accomplished [5–10]. Also, reductive deposition of different heavy metals such as Pt, Au and Rh was achieved by irradiation of semiconductor photocatalysts [11, 12].

Several oxides exhibit band-gap energies adequate for catalyzing the degradation of organic materials. Among them, TiO_2 has proven to be the most effective catalyst for detoxification of organic pollutants. Photochemical excitation of semiconductors leads to the formation of an electron-hole pair (e^-/h^+). This exciton can recombine and dissipate the energy. Alternatively, the electron (or hole) can be trapped by suitable chemical scavengers, i.e., electron acceptors (or electron donors), or eventually, surface defect states. In order to compete with the e^-/h^+ recombination, and trap effectively the conduction band electron, or the valence band hole, the respective acceptor or donor should be confined to the semiconductor surface. Various means to control the interfacial electron transfer at semiconductor-solution interfaces were developed. These include the encapsulation of electron acceptors in receptor-functionalized semiconductors [13], the electrostatic association of electron acceptors at the semiconductor surface [14], and the immobilization of semiconductor photocatalysts in redox-functionalized polymers [15, 16].

The mechanisms of photocatalytic degradation of organic materials in aqueous media or in a gaseous atmosphere, has been a subject of extensive studies [17]. Although the detailed routes leading to the mineralization of organic materials require further research efforts, it is clear that superoxide and specifically hydroxyl radicals (·OH) act as active reagents for the mineralization of the organic compounds [18]. These radicals are formed

* I. Willner and K. T. Ranjit, Israel Patent Application No. 121877, October 1, 1997.

‡ Author to whom all correspondence should be addressed.

by the scavenging of the e^-/h^+ by molecular oxygen and water, Equations 1–4.

$$O_2 + e^-_{c.b.} \rightarrow O_2^-\cdot \quad (1)$$

$$H_2O + h^+ \rightarrow OH\cdot + H^+ \quad (2)$$

$$OH\cdot + OH\cdot \rightarrow H_2O_2 \quad (3)$$

$$H_2O_2 + O_2^-\cdot \rightarrow \cdot OH + OH^- + O_2 \quad (4)$$

Insertion of ·OH into C—H bonds or functionalized C—H bonds, leads ultimately to the mineralization of the organic substances. Indeed, complete mineralization of, for example, a variety of aliphatic or aromatic chlorinated compounds was reported [19–21]. The reactive hydroxyl radicals might, however, dissipate by geminate coupling to yield H_2O_2. This leads to inefficient degradation of the pollutants. For improved degradation of the pollutant, the organic material should be preconcentrated at the semiconductor surface in order to effectively trap the respective radicals. Concentration of organic pollutants at semiconductors was accomplished by the surface modification of the photocatalyst with chelating agents [20] or by the immobilization of hydrophobic layers [21]. Also, surface modification of the catalyst with electron acceptor groups that concentrate electron-donor pollutants *via* the formation of donor-acceptor complexes [22] and the selective doping of the crystalline semiconductor oxide [23–25] proved to concentrate the pollutants at the photocatalyst surface and to enhance their degradation yields.

Lanthanide-ions are known for their ability to form complexes with various Lewis bases, (e.g. acids, amines, alcohols, aldehydes, thiols, etc.) *via* the interaction of these functional groups with f-orbitals of the lanthanides. This property is used in NMR spectroscopy, where the magnetic features of Eu^{3+} or Pr^{3+} yield significant chemical shift changes in the protons of the ion-associated organic ligands [26, 27]. Thus, the incorporation of lanthanide ions in a TiO_2 matrix could provide a means to concentrate the organic pollutant at the semiconductor surface.

The sol-gel method enables the synthesis of high surface area TiO_2 particles [28, 29] and nanometer size semiconductor colloids [30]. Here we wish to report on the preparation of lanthanide oxide-doped TiO_2. We describe the enhanced photodegradation of a series of aromatic compounds by the lanthanide-modified TiO_2 as compared to the non-modified photocatalyst [31]. The routes that lead to the enhanced activity of the europium-, praseodymium- and ytterbium-oxide-doped TiO_2 are discussed.

2. Experimental section

The non-modified TiO_2, europium-(Eu^{3+}), praseodymium (Pr^{3+}) and ytterbium (Yb^{3+})- doped TiO_2 were prepared as shown in Scheme 1. A sol of Ti(IV) isopropoxide, 7.38 ml in 10 ml methanol was prepared by mixing. After 15 min, a solution that contained methanol, 10 ml and conc. aq. HCl, 120 μl, was slowly added to the sol and the mixture was allowed to yield

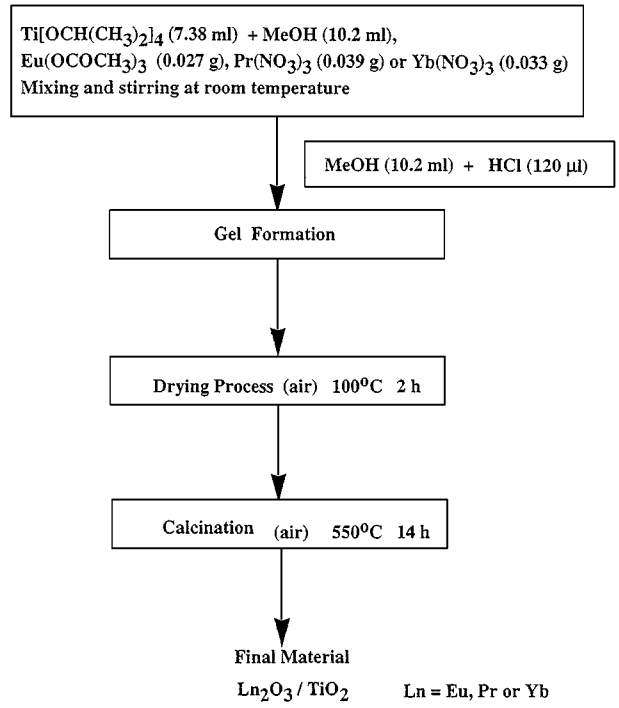

Scheme 1

the gel for 60 min. The resulting gel was dried at 100 °C for 2 h. The resulting TiO_2 powder was calcined to the anatase form by heating to 550 °C for 14 h in air. The europium, praseodymium and ytterbium-doped TiO_2, Eu_2O_3/TiO_2, Pr_2O_3/TiO_2 and Yb_2O_3/TiO_2 were prepared by a similar method, except that europium acetate, $Eu(OAc)_3$, praseodymium nitrate, $Pr(NO_3)_3$ and ytterbium nitrate, $Yb(NO_3)_3$ were dissolved in the sol prior to formation of the respective gels. The molar ratio of Ti(IV) to Eu(III), Pr(III) or Yb(III) is usually 100. Photocatalysts with a molar ratio of Ti(IV) and Eu(III) corresponding to Ti/Eu = 20, were also prepared.

The X-ray diffractograms of the calcined samples were recorded using a Philips PW 1050 powder diffractometer. The diffraction patterns were recorded at room temperature using a Ni filtered CuK_α radiation ($\lambda = 1.5418$ Å) for the samples. A scanning speed of 2 deg/min and a chart speed of 13 mm/deg were generally employed.

The surface area of the lanthanide-doped TiO_2 and the non-modified TiO_2 catalyst were measured by nitrogen adsorption at −196 °C by the dynamic BET method using a Micromeritics II 2370 surface area analyzer. The Transmission Electron Micrographs of the samples were recorded using a JEOL, JEM-100 CX, electron microscope operating at an accelerating voltage of 80 kV.

X-ray Photoelectron Spectroscopy, (XPS) analyses were performed with an AXIS-HS Kratos instrument using a monochromatized Al (K_α) source ($h\nu$ = 1486.6 eV). A flood gun was used to neutralize the sampled surface, while the C (1 s) line was used for a final energy scale calibration.

Photochemical degradation of organic substrates: *p*-nitrobenzoic acid (**1**), *p*-chlorophenoxyacetic acid (**2**), aniline, (**3**), salicylic acid (**4**) and *trans*-cinnamic

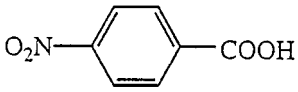

(1)

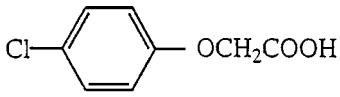

(2)

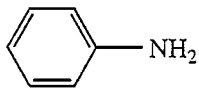

(3)

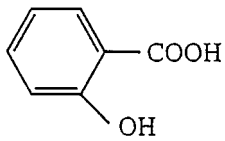

(4)

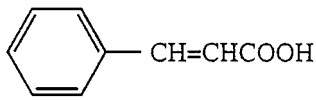

(5)

acid (**5**), were examined. Aqueous solutions of the respective pollutant, 2×10^{-5} to 3.5×10^{-4} M and 2.0 to 2.4 mg of the respective photocatalyst, were placed in a quartz cuvette. The suspension was irradiated with a 200 W Xe (Hg) lamp (Oriel). The cuvette was purged with oxygen during irradiation. After irradiation, the suspension was filtered and the solution analyzed spectroscopically (Uvikon-860, Kontron spectrophotometer).

2.1. DOC analyses

The analysis of DOC (Dissolved Organic Carbon) was carried out using a Dohrmann DC-190 TOC (Total Organic Carbon) analyzer ($T = 680\,^{\circ}$C) from Rosemount Analytical. The organic components were oxidized in an oxygen atmosphere at a platinum/alumina contact. The amount of carbon dioxide formed was measured using a non-dispersive IR-detector. The (TOC) Total Organic Carbon content was analyzed in this manner and the Inorganic Carbon Content was subtracted from this value. The latter is obtained by treating the samples with concentrated phosphoric acid. The calibration was performed using salicylic acid, oxalic acid and potassium hydrophthalate (KHP). All calibration samples could be fitted with a linear calibration curve. The samples were injected three consecutive times (injection volume, 50 μl) and the average values are reported.

2.2. GC-MS/FTIR-analysis

For the qualitative and quantitative analysis of the reaction products generated during time intervals of photolysis, the filtered samples (2 μl) were injected into a GC (HP 5971A MSD, mass selective detector), coupled with a HP 5965B ID (infrared detector). An HP-INNOWAX capillary column (cross-linked polyethylene glycol) was employed. All reaction products were identified by a combination of MS and FTIR-spectroscopy in comparison with analytical data bases. Furthermore, the calibration curves for the compounds investigated were also analyzed. In all cases, linear dependence of both MS and FTIR areas were obtained.

3. Results and discussion

The europium-, praseodymium- and ytterbium-modified TiO_2, Eu_2O_3/TiO_2, Pr_2O_3/TiO_2, Yb_2O_3/TiO_2 and non-modified TiO_2, were prepared by the general method outlined in Scheme 1. The molar ratio of Ti(IV) : Ln(III) prior to formation of the gel is usually 100 : 1. In a single system, a gel with the composition Ti(IV) : Eu(III) corresponding to 20 : 1 was prepared. The samples, after calcination, were analyzed by means of XRD and XPS.

The X-ray diffractograms of the samples reveal that in the bare titanium dioxide, the anatase phase is the major constituent of the photocatalyst (ca. 80%) accompanied by a rutile phase (ca. 20%). In the case of Eu_2O_3/TiO_2 and Yb_2O_3/TiO_2 catalysts, the anatase phase is predominant (>95%), while in the case of the Pr_2O_3/TiO_2 catalyst, the X-ray diffractogram reveals the presence of only the anatase phase. The surface area of the non-modified TiO_2 catalyst is 78.1 m^2/g. The surface areas of the Eu_2O_3/TiO_2, Pr_2O_3/TiO_2 and the Yb_2O_3/TiO_2 catalysts, are 102.1 m^2/g 125.0 m^2/g and 55.4 m^2/g, respectively. The TEM pictures indicate the particle sizes to be in the range 40–80 nm for the bare titanium dioxide. For the Eu_2O_3/TiO_2, Pr_2O_3/TiO_2 and the Yb_2O_3/TiO_2 catalysts, the particle sizes are in the range, 30–50 nm, 25–40 nm and 40–80 nm, respectively. The XPS measurements reveal that the lanthanides exist in the resulting TiO_2 photocatalysts as oxides, Ln_2O_3. Lanthanide concentrations were evaluated from their 3d (where available) and 4d lines. The europium-doped TiO_2 photocatalysts, having a molar ratio of Ti/Eu = 20 and Ti/Eu = 100, show a characteristic band at 1134.7 eV due to the Eu^{3+} ion. The band characteristic of Ti^{4+} appears at 458.6 eV. The ratio of the atomic concentration of Ti/Eu in the doped Eu_2O_3/TiO_2 photocatalyst (starting molar composition, Ti/Eu = 20) at the surface was evaluated to be ca. 20 $\pm$ 2, in full agreement with the molar ratio of the ions used in the preparation of the photocatalyst prior to the calcination. However, for the catalyst Eu_2O_3/TiO_2 (starting molar composition Ti/Eu = 100) the ratio of the Ti/Eu at the surface was evaluated to be ca. 40 $\pm$ 4 from XPS studies. This ratio is ca. 2.5 times lower than the molar ratio of the ions used in the preparation of the photocatalyst. Thus, it seems that there is an enrichment of Eu^{3+} at the surface due to the segregation of Eu_2O_3 to the surface after calcination. An additional

europium signal around 1125 eV was observed in the Eu_2O_3/TiO_2 samples, associated with the reduced form of the europium. It is believed that this metallic signal is induced by X-ray beam during the measurement. The magnitude of the signal ranged from 20 to 35% of the total europium signal for the Ti/Eu = 20 and Ti/Eu = 100 photocatalysts, respectively. In fact, it was inspected as a function of the X-ray irradiation time, showing a rough proportionality trend (note that due to the low concentration of the lanthanide, low irradiation exposures could not yield satisfactory signal-to-noise ratios). The XPS analysis of the Yb_2O_3/TiO_2 photocatalyst reveals a signal at approximately 185.5 eV due to Yb^{3+} (4d) with a Ti/Yb ratio that corresponds to 200 ± 50. In the case of the Pr_2O_3/TiO_2 photocatalyst, the signal due to Pr^{3+} (3d) appears at 933.5 eV. The Ti/Pr ratio is estimated to be 1000, but in this case the signal-to-noise ratio of Pr^{3+} signal was extremely low, so much so that the relative error could be as high as 100%. Contrary to the Eu_2O_3/TiO_2 photocatalyst, the photocatalysts Yb_2O_3/TiO_2 and Pr_2O_3/TiO_2 show a lower surface concentration of the Ln^{3+} ions as compared to the concentration used in the preparation of the gel. The XPS results clearly reveal that the lanthanide ions exist as their respective oxides.

The photodegradation of a series of organic aromatic compounds in aqueous solutions, e.g., *p*-nitrobenzoic acid, (**1**), *p*-chlorophenoxyacetic acid, (**2**), aniline, (**3**), salicylic acid, (**4**) and *trans*-cinnamic acid, (**5**), by Eu_2O_3/TiO_2, Pr_2O_3/TiO_2 and Yb_2O_3/TiO_2 was examined and compared to the photodegradation yields of these substrates by non-modified TiO_2. Fig. 1(A) shows the absorbance spectra of the *p*-nitrobenzoic acid (**1**) solution at time intervals of irradiation with the non-modified TiO_2 photocatalyst. A gradual decrease in the absorbance of the substrate is observed, indicating its photodegradation. Fig. 1(B) and Fig. 1(C) show the absorbance spectra of the (**1**) solution at time-intervals of irradiation in the presence of the Eu_2O_3/TiO_2 and Pr_2O_3/TiO_2, respectively. The substrate (**1**) is degraded at an impressive rate in the presence of Eu_2O_3/TiO_2 and Pr_2O_3/TiO_2 as compared to the non-modified TiO_2.

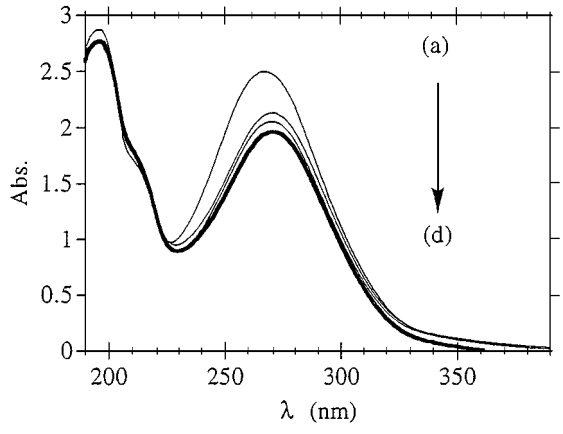

Figure 1(A) Absorption spectra of an aqueous *p*-nitrobenzoic acid (**1**) solution (2.4×10^{-4} M) (a) before irradiation, (b) after 30 min of irradiation, (c) after 45 min of irradiation, and (d) after 60 min of irradiation in the presence of non-modified TiO_2 photocatalyst (2.4 mg in 2.5 ml of solution).

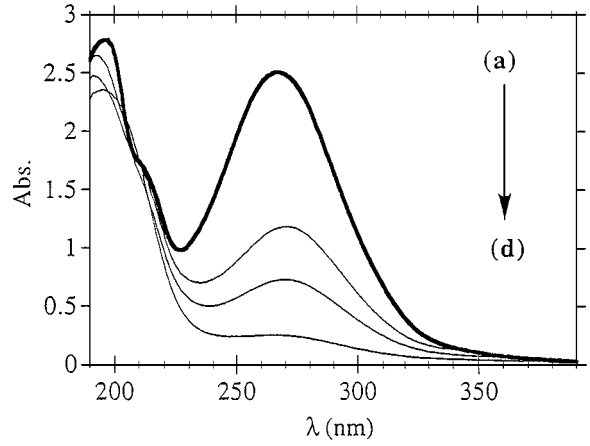

Figure 1(B) Absorption spectra of an aqueous *p*-nitrobenzoic acid (**1**) solution (2.4×10^{-4} M) (a) before irradiation, (b) after 30 min of irradiation, (c) after 45 min of irradiation, and (d) after 60 min of irradiation in the presence of Eu_2O_3/TiO_2 photocatalyst (Ti/Eu = 100), (2.2 mg in 2.5 ml of solution).

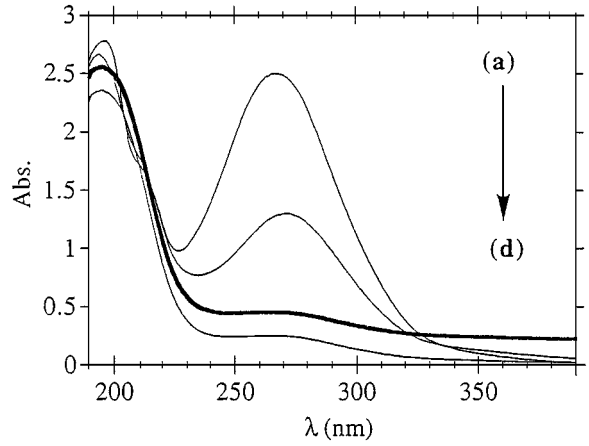

Figure 1(C) Absorption spectra of an aqueous solution of *p*-nitrobenzoic acid, (**1**), (2.4×10^{-4} M) (a) before irradiation, (b) after 30 min of irradiation, (c) after 45 min of irradiation, and (d) after 60 min of irradiation in the presence of the Pr_2O_3/TiO_2 photocatalyst (Ti/Pr = 100) (2.5 mg in 2.5 ml of solution).

For example, after 30 min of irradiation, only 18% of (**1**) are degraded by the non-modified TiO_2 whereas 54% and 50% of (**1**) are degraded by the Eu_2O_3/TiO_2 and Pr_2O_3/TiO_2, respectively. After 1 h of irradiation, ca. 32% of (**1**) are degraded by the non-modified TiO_2 while 90% and 80% are degraded by the Eu_2O_3/TiO_2 and Pr_2O_3/TiO_2, photocatalysts respectively. The concentrations of the solution were also monitored by GC-MS analyses. An excellent correlation was observed between the results obtained from UV-Vis spectra and GC-MS studies. For example, Fig. 2 shows the rate of photodegradation of (**1**) by Eu_2O_3/TiO_2 catalyst as assayed by spectroscopic analysis (curve a) and GC-MS (curve b), respectively and the rates of light-induced degradation of (**1**) by the non-modified TiO_2 catalyst by the same analytical methods, curve (c) and (d), respectively. It can be realized that the spectroscopic assay of the degradation rates of the substrate (**1**) coincides with the results obtained by GC-MS analysis of the irradiated samples. The photodegradation of (**1**) by the europium-modified titanium dioxide catalyst leads to the complete mineralization of the substrate.

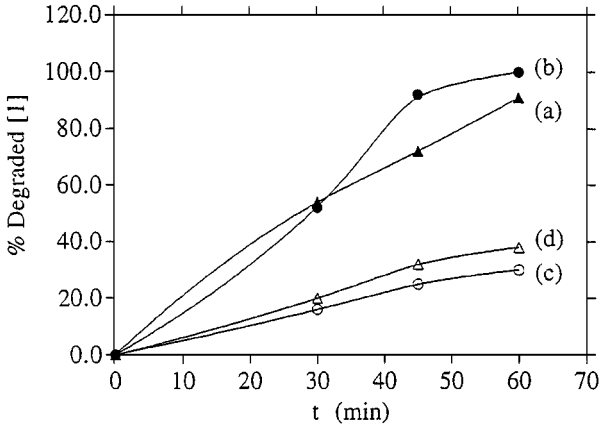

Figure 2 Rate of photodegradation of *p*-nitrobenzoic acid, (**1**), (2.4×10^{-4} M), in the presence of Eu_2O_3/TiO_2 photocatalyst; (a) assayed spectroscopically (b) analysed by GC-MS analysis. Photodegradation of (1), (2.4×10^{-4} M) in the presence of non-modified TiO_2 photocatalyst, (c) assayed spectroscopically and (d) analysed by GC-MS analysis. In all experiments 2.2–2.5 mg of the respective catalyst in 2.5 mL of solution were used.

This is evident from the fact that no new aromatic intermediates are observed in the GC-MS analysis of the irradiated samples [31].

To account for the enhanced photocatalytic activity of Eu_2O_3/TiO_2 and Pr_2O_3/TiO_2 as compared to the non-modified TiO_2, the adsorption of (**1**) to the modified and non-modified TiO_2 was examined. The amount of (**1**) adsorbed onto the photocatalyst was found to increase as the bulk concentration of the substrate is elevated and reaches a saturation value that corresponds to the maximum loading of (**1**) on the photocatalyst. For unmodified TiO_2, the saturation value of ca. 3.5×10^{-7} mol·g^{-1} of (**1**) on the catalyst is obtained at a bulk concentration of ca. 7×10^{-4} M of (**1**). For Eu_2O_3/TiO_2 and Pr_2O_3/TiO_2, the saturation value for the amount of adsorbed (**1**) is ca. 5.5×10^{-7} mol·g^{-1}. The respective adsorption isotherms were analyzed according to Langmuir's theory [32]. The derived adsorption constants of (**1**) on unmodified TiO_2 is $K_{ads} = 9.8 \times 10^2$ M^{-1}, while the adsorption constants of (**1**) to Eu_2O_3/TiO_2 and Pr_2O_3/TiO_2 are $K_{ads} = 2.1 \times 10^3$ M^{-1} and $K_{ads} = 2.8 \times 10^3$ M^{-1}, respectively. The adsorption constants of (**1**) to the lanthanide-ion-modified TiO_2 is ca. 3-fold higher as compared to the association of the substrate to TiO_2. This can be attributed to the formation of Lewis acid-base complexes between the Pr and Eu ions in the modified TiO_2 and the carboxylic acid residue of the substrate. Concentration of the substrate at the photocatalytic surface could then provide the mechanism for the enhanced mineralization of (**1**) by the modified photocatalysts. The photodegradation of *p*-chlorophenoxyacetic acid (**2**) was similarly found to be enhanced in the presence of the lanthanide-doped TiO_2 as compared to the process with non-modified TiO_2. After 1 h of irradiation only 34% of (**2**) are degraded by TiO_2, and ca. 85, 90 and 85% of (**2**) are mineralized by Eu_2O_3/TiO_2, Pr_2O_3/TiO_2 and Yb_2O_3/TiO_2, respectively. Analyzing the adsorption constants of (**2**) on the lanthanide-doped TiO_2 and non-modified TiO_2 reveals similarly enhanced association to the modified photocatalysts. The adsorption constants of (**2**) to TiO_2 is $K_{ads} = 4.5 \times 10^2$ M^{-1} while the adsorption constants of (**2**) to Eu_2O_3/TiO_2, Pr_2O_3/TiO_2 and Yb_2O_3/TiO_2 are $K_{ads} = 1.15 \times 10^3$ M^{-1}, $K_{ads} = 1.23 \times 10^3$ M^{-1} and $K_{ads} = 9.96 \times 10^2$ M^{-1}, respectively.

The activity of the Eu_2O_3/TiO_2 is preserved. After photodegradation of (**2**) with the photocatalyst, in the first run, the Eu_2O_3/TiO_2 catalyst was centrifuged and used for a second run. No noticeable degradation in the photocatalytic activity was observed.

The enhanced degradation yields of carboxylic acid derivatives in the presence of Eu_2O_3/TiO_2, Pr_2O_3/TiO_2 and Yb_2O_3/TiO_2 is general, and mineralization of salicylic acid (**4**) and *trans*-cinnamic acid (**5**) is substantially faster in the presence of the modified catalysts. The photodegradation of salicylic acid (**4**) was found to be enhanced in the presence of lanthanide-doped TiO_2 as compared to non-modified TiO_2. After 1 h of irradiation only 50% of (**4**) are degraded by non-modified TiO_2 whereas ca. 90, 95 and 92% of (**4**) are mineralized by Eu_2O_3/TiO_2, Pr_2O_3/TiO_2 and Yb_2O_3/TiO_2, respectively. The results obtained from the GC-MS analysis and the spectroscopic analysis for the Pr_2O_3/TiO_2 catalyst is shown in Fig. 3. It can be realized that the spectroscopic assay of the degradation rates of the substrate (**4**) coincides with the results obtained by GC-MS analysis of the irradiated samples. Fig. 4 shows the absorption spectra of the aqueous solution of *trans*-cinnamic acid, (**5**), upon irradiation for 45 min. in the presence of non-modified TiO_2 (curve b), and with Pr_2O_3/TiO_2 (curve c), Yb_2O_3/TiO_2 (curve d) and Eu_2O_3/TiO_2 (curve e). While 54% of the substrate are decomposed by the non-modified TiO_2 ca. 90, 93 and 95% of (**5**) are degraded by Pr_2O_3/TiO_2, Yb_2O_3/TiO_2 and Eu_2O_3/TiO_2, respectively.

The photodegradation of aniline, (**3**), was also examined in the presence of the different photocatalysts. Fig. 5 shows the absorption spectra of the aqueous aniline solution upon irradiation for 90 min. in the presence of non-modified TiO_2 (curve b) and in the presence of Pr_2O_3/TiO_2 (curve c) and Eu_2O_3/TiO_2 (curve d), respectively. Visually, the aniline solution irradiated in the presence of non-modified TiO_2 turned yellow, whereas the solutions treated with Eu_2O_3/TiO_2 and Pr_2O_3/TiO_2

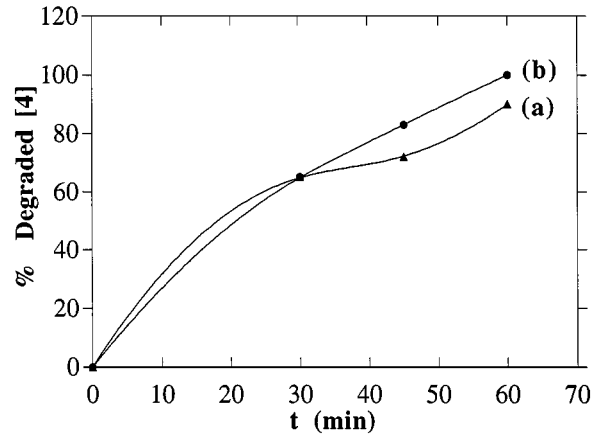

Figure 3 Rate of photodegradation of salicylic acid, (**4**), (2.4×10^{-4} M), in the presence of Pr_2O_3/TiO_2 photocatalyst; (a) assayed spectroscopically (b) analysed by GC-MS analysis. In all experiments 2.2–2.5 mg of the respective catalyst in 2.5 mL of solution were used.

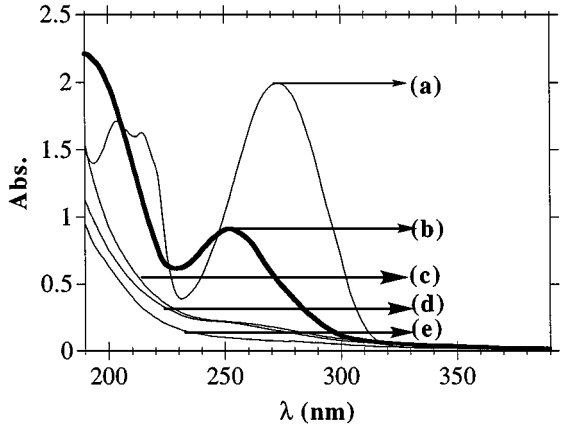

Figure 4 Absorption spectra of an aqueous solution of *trans*-cinnamic acid, (**5**), (2.2×10^{-5} M) (a) before irradiation, (b) after irradiation in the presence of TiO_2 catalyst for 45 min, (c) after irradiation in the presence of Pr_2O_3/TiO_2 catalyst for 45 min, (d) after irradiation with Yb_2O_3/TiO_2 catalyst for 45 min and (e) after irradiation with Eu_2O_3/TiO_2 catalyst for 45 min. In all experiments 2.2–2.5 mg of the respective catalyst in 2.5 ml of solution were used.

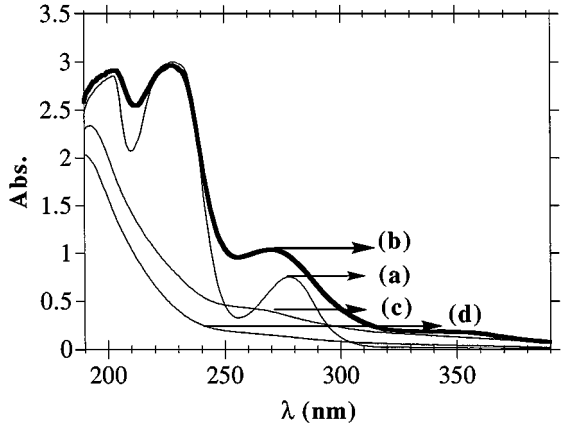

Figure 5 Absorption spectra of an aqueous solution of aniline, (**3**), (3.4×10^{-4} M) (a) before irradiation, (b) after irradiation in the presence of TiO_2 catalyst for 90 min, (c) after irradiation with the Pr_2O_3/TiO_2 photocatalyst for 90 min, and (d) after irradiation over Eu_2O_3/TiO_2 photocatalyst for 90 min. In all experiments 2.2–2.5 mg of the various catalysts in 2.5 ml of solution were used.

remained colorless after irradiation. Inspection of the absorbance spectra of the irradiated aniline solution in the presence of non-modified TiO_2 (Fig. 5, curve b) reveals the formation of at least a new intermediate with an absorbance maximum at $\lambda = 265$ nm and a tailing absorbance with a shoulder in the region $\lambda = 300$–420 nm. The latter absorbance yields the apparent yellow color of the solution and is presumably due to intermediate diazo dyes or oxidation products of aniline. The broad absorption spectra in the region 230–400 nm upon irradiation of the sample (**3**) with non-modified TiO_2, and the formation of the new intermediate, $\lambda_{max} = 265$ nm, are indicative of the formation of aromatic intermediates (presumably phenol). In contrast, the photodegradation of (**3**) with Eu_2O_3/TiO_2 leads to complete mineralization of aniline. With Eu_2O_3/TiO_2 the extent of mineralization of (**3**) is estimated to be >85% after one hour of irradiation.

Lanthanide ions themselves exhibit absorbance and emission features [33]. In order to verify whether the lanthanide-oxides participate in the light collection, energy transfer to TiO_2, or the photodegradation processes of the pollutants, we compared the photodegradation rate of *p*-chlorophenoxyacetic acid (**2**) by Eu_2O_3/TiO_2 photocatalysts that include Ti : Eu ratio of 100 and 20. Fig. 6 shows the rate of photodegradation of (**2**) by the two Eu_2O_3/TiO_2 photocatalysts. We see that the rate of degradation of (**2**) is *slower* in the presence of the Eu_2O_3/TiO_2 photocatalyst (Ti/Eu = 20) as compared to the photocatalyst consisting of Ti/Eu = 100. Thus, the relative content of TiO_2 and lanthanide oxide seems to control the effectiveness of the resulting photocatalyst. The fact that the Eu_2O_3/TiO_2 photocatalyst (Ti/Eu = 20) is less efficient than the catalyst (Ti/Eu = 100) is clearly indicative that the improved adsorption of the pollutants to the europium-oxide-doped photocatalysts is not the sole mechanism that controls the activity of the novel photocatalyst, as the adsorption of (**2**) is slightly higher on the Ti/Eu = 20 photocatalyst. The lower yield of the degradation of (**2**) by the Eu_2O_3/TiO_2 (Ti/Eu = 20) photocatalyst can be attributed to a light filtering effect since the europium oxide absorbs a part of the light that activates the TiO_2 semiconductor. This internal light filter effect is evident upon comparison of the light absorbed by the two Eu_2O_3/TiO_2 photocatalysts. We find that the Eu_2O_3/TiO_2 (Ti/Eu = 20) absorbs ca. 15–18% more of the incident light as compared to the Eu_2O_3/TiO_2 (Ti/Eu = 100). It should be noted that the absorbance of the Eu_2O_3/TiO_2 (Ti/Eu = 100) photocatalyst is higher by only ca. 5% as compared to the non-modified TiO_2 and hence the light filtering effect with this catalyst is negligible.

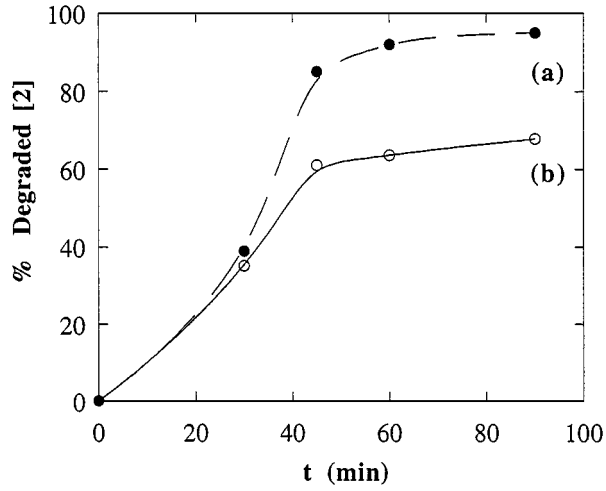

Figure 6 Degradation of *p*-chlorophenoxyacetic acid, (**2**), (3×10^{-4} M), over (a) Eu_2O_3/TiO_2 photocatalyst, 2.1 mg (Ti/Eu = 100), (b) Eu_2O_3/TiO_2 photocatalyst, 2.5 mg (Ti/Eu = 20) at time intervals of irradiation.

The elucidation of the mechanism leading to the enhanced activity of the lanthanide oxide-modified titanium dioxide as compared to non-modified TiO_2 photocatalyst is discussed henceforth. The crystalline phase of the TiO_2 catalyst is important in controlling its photoactivity, and previous reports have indicated that the rutile phase is less active [34, 35] and in some cases inactive [36, 37] in the photodegradation of organic compounds. While, the lanthanide-oxide-modified TiO_2 photocatalysts exist in the anatase phase, the non-modified TiO_2 photocatalyst includes a rutile phase (ca. 20%). The significant differences in

the photocatalytic activities of the two heterogeneous photocatalysts cannot be attributed to the differences in the structural composition between them. The surface areas of the heterogeneous photocatalysts could further influence the photodegradation yields. The surface areas of the Eu_2O_3/TiO_2, Pr_2O_3/TiO_2 and Yb_2O_3/TiO_2 are 102.1, 125.0 and 55.4 m^2/g, respectively, while the surface area of the non-modified TiO_2 is 78.1 m^2/g. The surface area of the Eu_2O_3/TiO_2 and Pr_2O_3/TiO_2 catalysts are ca. 30% and 60% high compared to the non-modified TiO_2 catalyst, whereas, the surface area of the Yb_2O_3/TiO_2 catalyst, is ca. 25% lower. However, the photocatalytic activity exhibited by Yb_2O_3/TiO_2 catalyst is comparable to that shown by Eu_2O_3/TiO_2 and Pr_2O_3/TiO_2 catalysts. Thus, the differences in the surface area cannot be a factor in influencing the photocatalytic activity. Modification of TiO_2 with altervalent cations could affect its bulk electronic structure (position of Fermi energy level and surface properties such as thickness of space charge layer, existence and concentration of surface states). That is, the work function of the doped semiconductor is increased and hence the Fermi energy level is shifted to lower values. Thus, the position of the flat band potential is shifted anodically. Consequently, on contact with an electrolyte, the depletion layer of the *p*-donor-doped semiconductor becomes thicker while the surface barrier is lowered as compared to the non-doped semiconductor. As a result, the capacity of the space charge region to separate the electron-hole pair is reduced. Thus, when TiO_2 is doped with a *p*-type donor, the activity is expected to decrease. However, the non-modified TiO_2 exhibits lower activity compared to the lanthanide-doped TiO_2. The equilibrium dark adsorption of the organic pollutants was found to be higher on the lanthanide-modified titanium dioxide catalysts as compared with that of the non-modified catalyst. This can be attributed to the formation of Lewis acid-base complexes between the lanthanide ions and the functional group residue of the organic pollutant. Concentration of the pollutant at the photocatalytic surface could then provide the mechanism for the enhanced mineralization of (**1**)–(**5**) by the modified photocatalysts.

In conclusion, we have tailored a new class of photocatalysts for the degradation of functionalized organic substrates. The photocatalysts consist of lanthanide-oxide/TiO_2 composites. The present study has demonstrated that europium-, praseodymium- and ytterbium-oxide-doped TiO_2 exhibit impressively higher photocatalytic activities for degradation of organic pollutants. For all of the examined pollutants, and specifically for *p*-nitrobenzoic acid, (**1**), complete mineralization of the substrates was observed, without the formation of the pollutant-intermediates. As the photodegradation of the organic material involves oxidative mineralization, we suggest that the intermediate alcohols, aldehydes and carboxylic acids are tightly bound to the lanthanide ions, and their surface degradation prevents their appearance in solution. Our study has emphasized that the loading of the TiO_2 photocatalyst must be regulated. High loading of the photocatalyst with lanthanide ions decreases the photocatalytic activity of TiO_2 due to the absorbance of light by the lanthanide ion and screening of the band-gap photoexcitation of the catalyst.

Acknowledgement

This research is supported by the Israel Ministry of Science, MOS, Israel, and the Bundesministerium für Bildung, Wissenschaft, Forschung und Technologie (BMBF), Germany.

References

1. (a) D. F. OLLIS and H. AL-EKABI (eds.), "Photocatalytic Purification and Treatment of Water and Air" (Elsevier, Amsterdam, 1993); (b) T. WATANABE, A. KITAMURA, E. KOJIMO, C. NAKAYAMA, K. HASHIMOTO and A. FUJISHIMA, *Trace Met. Environ.* **3** (1993) 747; (c) K. SUZUKI, *ibid.* **3** (1993) 421; (d) M. A. FOX and M. T. DULAY, *Chem. Rev.* **93** (1993) 341; (e) D. M. BLAKE, Bibliography of work on the photocatalytic removal of hazardous compounds from water and air, NREL/TP-430-6084, National Renewable Energy Laboratory, Golden, Colorado; (f) A. MILLS and S. L. HUNTE, *J. Photochem. Photobiol. A: Chem.* **108** (1997) 1.
2. (a) A. MILLS, R. H. DAVIES and D. WORSLEY, *Chem. Soc. Rev.* **22** (1993) 417; (b) A. HELLER, *Acc. Chem. Res.* **28** (1995) 503; (c) R. W. MATTHEWS, *Pure Appl. Chem.* **64** (1992) 1285; (d) M. NAIR, Z. LUO and A. HELLER, *Ind. Chem. Eng. Res.* **32** (1993) 2318; (e) N. SERPONE and E. PELIZZETTI (eds.), "Photocatalysis" (Wiley, New York, 1989); (f) M. R. HOFFMANN, S. T. MARTIN, W. CHOI and D. W. BAHNEMANN, *Chem. Rev.* **95** (1995) 69; (g) A. L. LINSEBIGLER, G. LU and J. T. YATES JR., *ibid.* **95** (1995) 735.
3. M. DAROUX, D. KLVANA, M. DURAN and M. BIDEAU, *Can. J. Chem. Eng.* **63** (1985) 668.
4. M. FORMENTI, F. JUILLET, P. MERIAUDEAU and S. TEICHNER, *J. Chem. Technol.* (1971) 680.
5. G. MILLS and M. R. HOFFMANN, *Environ. Sci. Technol.* **27** (1993) 1681.
6. C. KORMANN, D. W. BAHNEMANN and M. R. HOFFMANN, *ibid.* **25** (1991) 494.
7. E. R. CARRAWAY, A. J. HOFFMAN and M. R. HOFFMANN, *ibid.* **28** (1994) 786.
8. A. CHEMESEDDINE and H. P. BOEHM, *J. Mol. Catal.* **60** (1990) 295.
9. J. C. D'OLIVEIRA, C. MINERO, E. PELIZZETTI and P. PICHAT, *J. Photochem. Photobiol. A: Chem.* **72** (1993) 261.
10. J. C. D'OLIVEIRA, G. AL-SAYYED and P. PICHAT, *Environ. Sci. Technol.* **24** (1990) 990.
11. (a) M. ALBERT, Y. M. GAO, D. TOFT, K. DWIGHT and A. WOLD, *Mater. Res. Bull.* **27** (1992) 961; (b) Y. INEL and D. ERTEK, *J. Chem. Soc., Farad. Trans.* **89** (1993) 129.
12. E. BORGARELLO, N. SERPONE, G. EMO, R. HARRIS, E. PELIZZETTI and C. MINERO, *Inorg. Chem.* **25** (1986) 4499.
13. (a) I. WILLNER and Y. EICHEN, *Y. J. Amer. Chem. Soc.* **109** (1987) 6862; (b) I. WILLNER, Y. EICHEN and A. J. FRANK, *J. Amer. Chem. Soc.* **111** (1989) 1884.
14. A. J. FRANK, I. WILLNER, Z. GOREN and Y. DEGANI, *J. Amer. Chem. Soc.* **109** (1987) 3568.
15. I. WILLNER, Y. EICHEN, A. J. FRANK and M. A. FOX, *J. Phys. Chem.* **97** (1993) 7264.
16. T. NAKAHIRA and M. GRÄTZEL, *ibid.* **88** (1984) 4006.
17. (a) C. D. JAEGER and A. J. BARD, *J. Phys. Chem.* **83** (1979) 3146; (b) S. TUNESI and M. A. ANDERSON, *Langmuir* **8** (1992) 487.
18. (a) S. YAMAZAKI-NISHIDA, S. CERVERA-MARCH, K. J. NAGANO, M. A. ANDERSON and K. HORI, *J. Phys. Chem.* **99** (1995) 15814; (b) J. FAN and J. T. YATES, JR., *J. Amer. Chem. Soc.* **118** (1996) 4686.
19. K. VINODGOPAL, S. HOTCHANDANI and P. V. KAMAT, *J. Phys. Chem.* **97** (1993) 9040.

20. C. MINERO, E. PELIZZETTI, S. MALATO and J. BLANCO, *Chemosphere* **26** (1993) 2103.
21. Y. MAO. C. SCHONEICH and K. D. ASMUS, *J. Phys. Chem.* **95** (1991) 80.
22. K. T. RANJIT, E. JOSELEVICH and I. WILLNER, *J. Photochem. Photobiol. A: Chem.* **96** (1996) 185.
23. W. LEE, Y. R. DO, K. DWIGHT and A. WOLD, *Mater. Res. Bull.* **28** (1993) 1127.
24. M. GRÄTZEL and R. F. HOWE, *J. Phys. Chem.* **94** (1990) 2566.
25. J. KIWI and M. GRÄTZEL, *ibid.* **90** (1986) 637.
26. (a) D. L. RABENSTEIN, *Anal. Chem.* **43** (1971) 1599; (b) J. P. SHOFFNER, *ibid.* **47** (1975) 341.
27. (a) R. E. RONDEAU and R. E. SIEVERS, *J. Amer. Chem. Soc.* **93** (1971) 1522; (b) J. K. M. SANDERS, S. W. HANSON and D. H. WILLIAMS, *ibid.* **94** (1972) 5325.
28. C. J. BRINKER and G. W. SCHERER, "The Physics and Chemistry of Sol-Gel Processing" (Academic Press, New York, 1990).
29. G. M. PAJONK, *Heter. Chem. Rev.* **2** (1995) 129.
30. (a) G. DAGAN and M. TOMKIEWICZ, *J. Phys. Chem.* **97** (1993) 12651; (b) E. JOSELEVICH and I. WILLNER, *ibid.* **98** (1994) 7628.
31. K. T. RANJIT, I. WILLNER, S. BOSSMANN and A. M. BRAUN, *Res. Chem. Intermed.*, in press (1999).
32. I. LANGMUIR, *J. Amer. Chem. Soc.* **40** (1918) 1361.
33. K. TENNAKONE, D. A. ILEPERUMA, J. M. S. BANDARA and C. T. K. THAMINIMULLA, *Sol. Energ. Mater.* **22** (1991) 319.
34. H. NODA, K. OIKAWA and H. KAMADA, *Bull. Chem. Soc. Jpn.* **66** (1993) 455.
35. B. OHTANI and S. NISHIMOTO, *J. Phys. Chem.* **97** (1993) 920.
36. A. MILLS, S. MORRIS and R. DAVIES, *J. Photochem. Photobiol. A: Chem.* **70** (1993) 183.
37. S. T. MARTIN, C. L. MORRISON and M. R. HOFFMANN, *J. Phys. Chem.* **98** (1994) 13695.

Received 29 July 1998
and accepted 27 April 1999